Modeling the Deviation of Water Flow from the Flow Line during Long-Distance Sprinkling

Zafar Khudayarov* [1], Tolib Khalmuradov[1], Madrakhim Allanazarov[1], Sherzodkhuja Mirzakhodjaev[1], Khusniddin Irisov[1]

[1]Tashkent State Agrarian University, Tashkent, 100140, Uzbekistan

hudayarovzafar5@gmail.com

Abstract. This article presents the results of a theoretical study on the deviation of water flow from the flow line in direct-flow sprinkling devices. The deviation of water flow from the flow line significantly affects its distribution over the field surface and the efficiency of sprinkling. The article also examines the forces acting on the water flow during sprinkling, the trajectory of the flow movement, and its mathematical model. In addition, analytical calculations of sprinkling intensity during long-distance sprinkling are carried out. The influence of the initial velocity of artificial droplets on the deviation of the water flow from the flow direction is studied.

Keywords: sprinkling, water flow, deviation angle, mathematical model, aerodynamic force, trajectory.

1 Introduction

In order to save water resources and irrigate agricultural crops efficiently, the sprinkling method is widely used. In particular, direct-flow long-distance sprinkling systems stand out in modern agricultural engineering for their high efficiency. At the same time, the deviation of water flow from the flow line leads to its uneven distribution in the fields, the formation of water layers of different thicknesses in the sprinkled area, and consequently has a negative impact on irrigation efficiency.

Although scientific literature provides information on the movement of water flow in the aerodynamic medium and the forces acting on it – centrifugal, Coriolis, and other forces – the deviation angle and deviation distance of water flow from the flow line in long-distance sprinkling have not been sufficiently analyzed [1]. Recent studies have also focused on mathematical modeling and optimization of sprinkler irrigation systems under various operating conditions [9–14]. In this regard, this article theoretically examines the deviation of water flow from the flow line, its influencing factors, and consequences. Based on a mathematical model, a method for determining the deviation angle, the trajectory of the flow, and the sprinkling intensity is proposed.

© The Author(s) 2026

A. M. Bozdoğan et al. (eds.), *Proceedings of the 5th International Conference on Research of Agricultural and Food Technologies (I-CRAFT 2025)*, Atlantis Highlights in Sustainable Development 8,
https://doi.org/10.2991/978-94-6239-666-1_11

2 Materials and methods

The sprinkling process is carried out using short-, medium-, and long-distance sprinkling devices. Long-distance sprinkling occurs under high pressure, with a large initial velocity of the water flow. In most cases, water flow is sprinkled onto the field surface using barrels equipped with nozzles of different diameters, which form a flow line. These nozzle barrels generate direct-flow sprinkling [1].

According to Yu.F. Snipich's studies, the expansion angle of the water flow is 3–4 degrees [2]. In A.P. Isaev's research, the length of the first section of the water flow was determined by the following formula [3]:

$$l_1 = 278{,}7 \div 2{,}1 \times 10^{-4} Re\, d_s\,, \text{ m.} \quad (1)$$

here, d_s – the diameter of the water droplet, Re – Reynolds number.

The flight distance of a water droplet ejected from the nozzle is given as:

$$L = l_1 + l_2 + l_3, \text{ m.} \quad (2)$$

Determining the trajectory of the water flow ejected from nozzle barrels has practical importance [4].

During the sprinkling process in crop fields, the barrels of long-distance sprinkling devices perform a reciprocating motion with an angular velocity ωω in the direction perpendicular to the machine's movement. This causes additional forces to act on the water flow and the water droplets.

The velocity of the water flow along the XZ axis (perpendicular to the direction of the machine's movement) depends on the reciprocating motion of the working organ and the relative motion generated around point A (see Fig. 1). To derive the mathematical model of the water flow movement along the XZ axis, the process is analyzed.

The sprinkling machine moves forward with velocity ϑ_m. The rotation center is located at point O, where the direct-flow sprinkling device rotates with angular velocity ω. The nozzle, situated at the end of a barrel of radius R (equal to the barrel length in this case), has a linear velocity ϑ_s and starts sprinkling from point O_0 along the OZ axis. The flow line is directed along line OB, and the sprinkling process takes place in the three sections mentioned above.

Based on the law of inertia, the continuity equation of fluid flow, surface tension force, hydrodynamics, Newton's second law, and other well-known physical principles, the motion of the water flow can be considered as a complex relative movement in the XYZ coordinate system.

At the beginning of the process, the rotation angle of the sprinkler barrel is φ=0°. As sprinkling begins, the angle φφ increases, and by the end of the process, it reaches 180°. The length of the water flow, l_1, is determined by Isaev's formula (1) and corresponds to distance AB in the diagram.

$$l_{1x} = (278{,}7 \div 2{,}1 \times 10^{-4} Re\, d_s) \cos\alpha \cos\varphi\,, \text{ m.} \quad (3)$$

$$l_{1z} = (278{,}7 \div 2{,}1 \times 10^{-4} Re\, d_s) \cos\alpha \sin\varphi\,, \text{ m.} \quad (4)$$

here, α – installation angle of the barrel relative to the horizontal (droplet launch angle).

In the graphs shown in Fig. 2**,** the lengths of the distance AB (the length of the first section of the water flow), calculated using formulas (3) and (4), are presented along the X and Z axes with respect to changes in the angle φ. Due to the stretching of the

water flow, the maximum length along the X-axis is l_1 x=0.12 m at φ=90°, while its projection along the Z-axis reaches l_1 z=0.32 m l_1 z=0.32m at φ=15°.

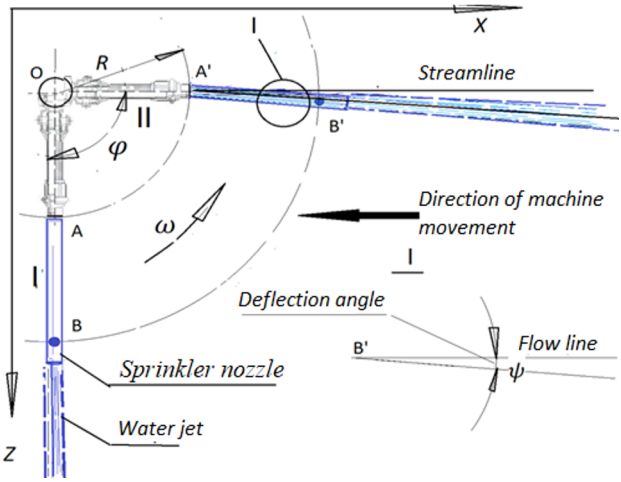

Fig. 1. Scheme of water flow deviation from the flow line in direct-flow sprinkling (top view of the sprinkling device).

The velocity component at point A has a speed of ϑ_A and forms an angle λ relative to the X-axis**.** The length of the water flow equals l_1=|AB|, with its center of gravity located at point B**.** According to the laws of dynamics, the water flow moves around point A with an angular velocity $\dot{\psi}$. As a result of this motion, the water flow centered at point B is subjected to centrifugal force with normal and tangential components, angular velocity $\dot{\psi}$, and the Coriolis force.

Due to the surface tension force of the liquid, a force arises that resists the stretching of the water flow, while the aerodynamic force of the surrounding medium acts in the opposite direction to the motion of the moving body. Under the influence of these forces, the water flow moving along the OB direction, with velocity components $\dot{\psi}$ and ϑ_A, forms an angle ψ and deviates from the horizontal plane by an angle λ+ψ, thereby moving along line OO" (Fig. 2).

The water flow, deflected by angle ψ, begins to break up after point B and continues its movement along line ABO". The resulting angle ψ represents the deviation of the water flow from the flow line, influencing its distribution across the field surface—a phenomenon that has not yet been sufficiently studied in research.

3 Results

Let us determine the coordinates of point B of the water flow in the coordinate system (Fig. 2):

$$X = R \cdot sin\varphi + l_1\, sin(\varphi - \psi)cos\alpha - \ \vartheta_m\, t; \tag{5}$$

$$Y = (R + l_1)\sin\alpha; \quad (6)$$

$$Z = R \cdot \cos\varphi + l_1 \cos(\varphi - \psi) cos\alpha. \quad (7)$$

here, R is the barrel length (m), l_1 is the length of the first section of the water flow (m), $\vartheta_m t$ is the distance traveled by the sprinkling device per unit time (m), φ is the rotation angle of the barrel (°), ψ is the deflection of the water flow around point A (°), and α is the installation angle of the barrel relative to the horizontal (°).

To solve this system of equations, it is necessary to determine the deflection angle ψ of the water flow from the flow line under the influence of acting forces.

Equations (5), (6), and (7) can be simplified as:

$$X = sin\varphi(R + l_1\ cos\psi\ cos\alpha) - l_1\ cos\varphi sin\psi\ cos\alpha - \vartheta_m t; \quad (8)$$

$$Y = (R + l_1)\sin\alpha; \quad (9)$$

$$Z = cos\varphi(R + l_1\ cos\psi\ cos\alpha) - l_1\ cos\varphi sin\psi\ cos\alpha\ . \quad (10)$$

First, we determine the velocity vectors. The velocity of point B, ϑ_B, according to the velocity addition theorem, is equal to the relative velocity of point A, ϑ_A, plus the translational velocity of the water flow's center of gravity at point B around point A, ϑ_s:

$$\overrightarrow{\vartheta_B} = \overrightarrow{\vartheta_A} + \overrightarrow{\vartheta_s}\ , \text{m/s}. \quad (8)$$

here, ϑ_s – velocity generated by the rotation of point B around point A, determined as:

$$\vartheta_s = l_1 \cdot \dot{\psi}, \text{ m/s}. \quad (9)$$

where l_1 – length of the first section of the water flow (determined by equation (1)); $\dot{\psi}$ – angular velocity of the water flow around point A.

The velocity of point A is determined by:

$$\vartheta_A = \sqrt{\vartheta_{sop}^2 + \vartheta_m^2 - 2\vartheta_{sop} \cdot \vartheta_m . sin\varphi}\ ;$$

Equation (8) can then be written as:

$$\vartheta_B^2 = \vartheta_A^2 + {l_s}^2 \cdot \dot{\psi}^2 - 2 \cdot \vartheta_A \cdot l_1 \cdot \dot{\psi} \cdot sin\gamma, \quad (10)$$

where: γ=180°−ψ−λ , λ – angle between velocity ϑ_A and the X-axis, determined by:

$$cos\lambda = \frac{\vartheta_A^2 + \vartheta_m^2 - \vartheta_{sop}^2}{\vartheta_A \cdot \vartheta_m}$$

or equivalently:

$$\lambda = arccos\left(\frac{\vartheta_m \cdot \vartheta_{sop} \cdot cos\varphi}{\sqrt{\vartheta_m^2 + \vartheta_{sop}^2 - 2\vartheta_m \cdot \vartheta_{sop} \cdot cos\varphi}}\right). \quad (11)$$

For long-distance sprinkling, the mathematical model of the water flow trajectory is constructed on the basis of Newton's second law, considering the projections of the forces acting on the water flow along the X and Z axes [5]:

$$m_s a_x = F_x\ , \quad (12)$$

$$m_s a_z = F_z\ . \quad (13)$$

The tangential and normal components take the following form:

$$m_s l_1 \ddot{\psi} = F_{air}^{\tau} - F_{in}^{\tau} + F_k + F_1; \quad (14)$$

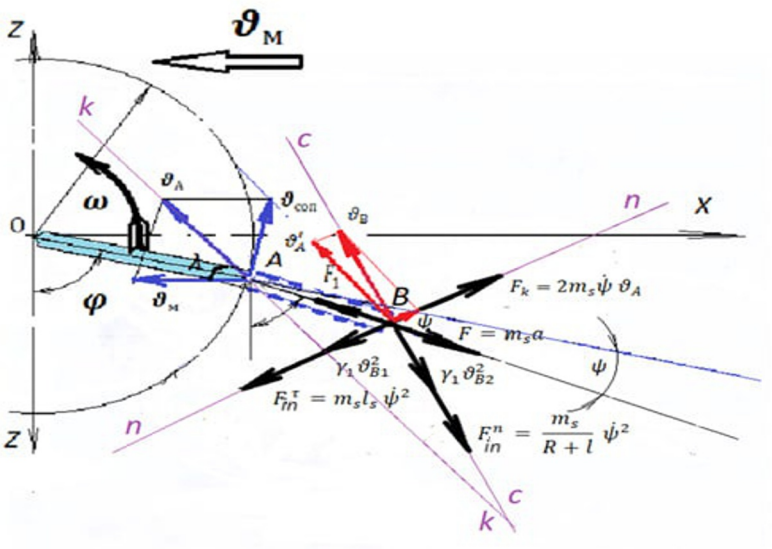

Fig. 2. Scheme for determining the forces acting on the water flow in the first section of direct-flow sprinkling

$$m_s \frac{\vartheta_B^2}{R+l_1} = -F_{air}^n - F_{in}^n. \quad (15)$$

Substituting, we obtain:

$$m_s l_1 \ddot{\psi} = -\gamma_1\ {l_1}^2\,\dot{\psi}^2\,cos\lambda\ \cdot sin\psi - m_s l_1\,\dot{\psi}^2\ + 2m_s\dot{\psi}\,\vartheta_A + c\Delta l; \quad (16)$$

$$m_s \frac{\vartheta_B^2}{R+l_1} = -\gamma_1\ {l_1}^2\,\dot{\psi}^2 \cos\psi - \frac{m_s}{R+l_1}\,\dot{\psi}^2. \quad (17)$$

Here:

$F_x = m_s a_x$, $F_z = m_s a_z$ – forces acting on the water flow at the nozzle due to hydrodynamic pressure, N;

$F_k = 2m_s\dot{\psi}\,\vartheta_A$ – Coriolis force, N;

$F_{in}^n = \frac{m_s}{R+l_1}\,\dot{\psi}^2$ – normal component of the centrifugal force, N;

$F_{in}^{\tau} = m_s l_1\,\dot{\psi}^2$ – tangential component of the centrifugal force, N;

$\gamma_1\vartheta_{B2}^2 = \gamma_1\ {l_1}^2\,\dot{\psi}^2\ \cos\psi$ – normal component of air resistance force, N;

$\frac{C_x\,\rho_m}{2}$, C_x, where C_x is the aerodynamic drag coefficient (Cx=0.5);

ρmρm is the air density, at t=20°C, ρ_m=1.2754 kg/m^3;

$\gamma_1\vartheta_{B1}^2 = \gamma_1\ {l_1}^2\,\dot{\psi}^2\ cos\lambda\ sin\psi$ – tangential component of air resistance force, N;

$F_l = c\Delta l$ – surface tension force resulting from the stretching of the water flow, N.

Similar numerical approaches have been applied in modeling irrigation jet dynamics and droplet trajectory analysis [15–20]. The second-order differential equation is written as:

$$l_1\ddot{\psi} + l_1\dot{\psi}^2 + \frac{\gamma_1 l_1}{m_s}\dot{\psi}^2 cos\lambda \cdot sin\psi = \frac{2\dot{\psi}\vartheta_A}{l_1} + \frac{c\Delta l}{m_s l_1}. \quad (18)$$

Equation (18) in simplified form is:

$$\ddot{\psi} = f(\psi, \dot{\psi}, t), \quad (19)$$

Where,

$$f(\psi, \dot{\psi}, t) = \frac{1}{l_1}\left[-\dot{\psi}^2 - \frac{\gamma_1 l_1}{m_s}\dot{\psi}^2 \cos\lambda \cdot \sin\psi + \frac{c\Delta l}{m_s l_1}\right]. \quad (20)$$

Equation (19) is solved using the Cauchy method (i.e., the 4th-order Runge–Kutta method). Introducing the following substitutions:

$$y_1 = \psi, \qquad y_2 = \dot{\psi}. \quad (21)$$

The system is transformed into first-order equations:

$$\begin{cases} y_1' = y_2; \\ y_2' = f(y_1, y_2, t). \end{cases} \quad (22)$$

Or equivalently:

$$y_1(t_{n+1}) = y_1(t_n) + \frac{1}{6}(k_1 + 2k_2 + 2k_3 + k_4); \quad (23)$$

$$y_2(t_{n+1}) = y_2(t_n) + \frac{1}{6}(l_1 + 2l_2 + 2l_3 + l_4, \quad (24)$$

For y1(t)y1(t), the intermediate slopes are calculated with step size h:

$$k_1 = h \cdot y_2(t_n);$$
$$k_2 = h \cdot \left[y_2(t_n) + \frac{1}{2}h \cdot f(y_1, y_2, t)\right];$$
$$k_3 = h \cdot \left[y_2(t_n) + \frac{1}{2}h \cdot f(y_1, y_2, t)\right];$$
$$k_4 = h \cdot \left[y_2(t_n) + \frac{1}{2}h \cdot f(y_1, y_2, t)\right]. \quad (25)$$

For $y_2(t)$, the intermediate slopes are:

$$l_1 = h \cdot f(y_1, y_2, t_n);$$
$$l_2 = h \cdot f\left(y_1 + \frac{k_1}{2}, y_2 + \frac{l_1}{2}, t_n + \frac{h}{2}\right);$$
$$l_3 = h \cdot f\left(y_1 + \frac{k_2}{2}, y_2 + \frac{l_2}{2}, t_n + \frac{h}{2}\right);$$
$$l_4 = h \cdot f(y_1 + k_3, y_2 + l_3, t_n + h) \quad (26)$$

The equation is solved under the initial condition $\varphi=0° \Rightarrow \psi=0°$. Based on differential equations (23) and (24), the graph of ψψ versus φφ is presented in Fig. 3.

The analysis of the obtained results shows that the value of the angle ψ changes within the range of $\psi = 0° \div 5.1°$ as the rotation angle of the barrel φ increases. The maximum value of ψ is reached at $\varphi = 150°$, where $\psi = 5.1°$. Naturally, this affects the distribution of the water flow on the field surface and the irrigation intensity.

By substituting the values of the deviation angle ψ of the water flow from the flow line, calculated by equation (15), into formulas (5), (6), and (7), the coordinates of point V of the water flow in section 1 of the irrigation process were determined as a function of the angle φ. Taking into account the equations of motion of the water droplet (8), (9), and (10), as well as (6) and (7), a mathematical model of the trajectory of the water droplet motion for direct-flow sprinkling devices is obtained. Previous computational investigations of droplet movement and environmental interaction effects have been reported in recent studies [21–26].

When the barrel angle changes within φ = 0–180°, the coordinates of the irrigated water flow along the X and Z axes at any moment are determined by the following equations [6]:

$$x(t_{i+1}) = x(t_i) + \vartheta_x(t_i)\Delta t; \quad (27)$$

$$y(t_{i+1}) = y(t_i) + \vartheta_y(t_i)\Delta t; \quad (28)$$

$$z(t_{i+1}) = z(t_i) + \vartheta_z(t_i)\Delta t. \quad (29)$$

From this, the variable coefficient of the medium for a moving water droplet is determined by the following expression:

$$K(t) = -\left(\frac{18\mu}{\rho_c d^2} + \frac{\rho_m C_x \sqrt{\vartheta_x{}^2(t)+\vartheta_z{}^2(t)+\vartheta_y{}^2(t)}}{4\rho_c d}\right) \quad (30)$$

where μ is the viscosity coefficient of the medium (for air μ = 1.8·10⁻⁵ Pa·s); d_s – diameter of the water droplet, m; $\vartheta^{\rightarrow}(t)$ – absolute value of the velocity vector of the body, m/s; ρmρm – density of the medium (for air at temperature t = 20 °C, ρ_m=1.2754 kg/m³).

Based on equations (27), (28), and (29), the coordinates of the water droplet were calculated for initial velocities ϑ_0=15 m/s and ϑ_0=25 m/s, with a barrel installation angle relative to the horizontal α = 30°, and water droplet diameter d = 2 mm. The changes of coordinates along the XZ axis and their dependence on the angle φ are presented in the graphs of Fig. 5. Next, the irrigation intensity in long-range sprinkling is calculated. To determine the irrigation intensity in direct-flow sprinkling, a scheme is constructed in the coordinate system, showing the barrel rotation by angle φ and, accordingly, the deviation of the water flow from the flow line by angle ψ (Fig. 2).

At point a_1, the barrel starts irrigation, and at point anan, it reaches the final boundary of its movement – this can be called the first cycle. The second cycle must begin from point anan in the reverse direction of movement.

In the first cycle, the barrel rotates by angle φ (in our case φ = 180°). In this state, the water flow line lags behind the barrel rotation angle by ψ (in our case ψ = 5°10″), occupying point O_i''. Since this state corresponds to the end of the cycle, the barrel stops momentarily and must begin the second cycle. At the moment when the barrel stops, its angular velocity caused by rotation around the center O becomes ω=0.

It is known that the forces arising at point V of the water flow are caused by the machine's velocity and the angular velocity of the barrel. When ω=0, all these forces become equal to 0, which means that at this instant the water flow line must coincide with the position at point anan starting from point O_i'. The distance ΔS between points O_i' and anan indicates that the irrigation intensity is equal to 0 along this distance. We call the distance ΔS the deviation distance of the water flow line.

The deviation distance of the water flow line ΔS is determined by the following expression:

$$\Delta S = (R \cdot \cos\varphi + l_1 \cos(\varphi - \psi)cos\alpha + z(t_i) + \vartheta_z(t_i)\Delta t\, cos\varphi)sin\psi \ . \quad (31)$$

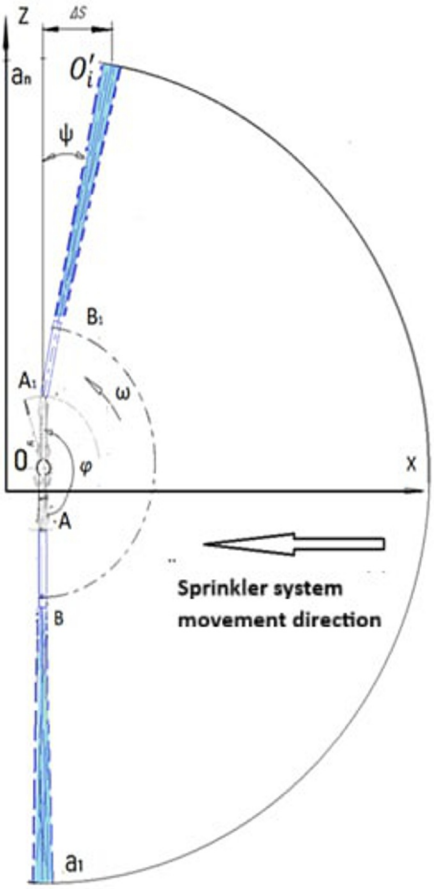

Fig. 3. Scheme for determining the deviation distance ΔS of the water flow line in straight-flow sprinkling

In the graph shown in Fig. 4, the dependence of the deviation distance ΔS of the water flow line on its initial velocity is presented. From the graph, it can be seen that the value of ΔS increases as the initial velocity of the water flow increases. This is explained by the fact that, with the increase of the initial velocity ϑ_0, the flight distance L of the water droplet also increases.

In the previous sections, we analyzed the factors influencing the flight distance of the water droplet. In this case as well, the same factors determine the flight distance.

From the calculation of formula (20), it can be concluded that the deviation distance ΔS of the water flow line also plays an important role in the irrigation intensity and in the distribution of water droplets on the field surface. Depending on the value of the initial velocity ϑ_0, ΔS ranges between 0.35–1.6 meters. This indicates that, in order

to ensure irrigation intensity in straight-flow sprinkling according to agrotechnical requirements, the deviation distance ΔS must be considered.

A.G. Vinogradov and O.M. Yakhno, based on the analysis of water flow velocity profiles, developed the following formula to calculate the spreading of the flow [7]:

$$0{,}22\ \bar{x} = \bar{b} + \frac{1}{\sqrt{\sigma}}\Big[ln\left(1{,}22 \cdot \bar{b} \cdot \sqrt{\sigma} + \sqrt{1 + 1{,}48 \cdot \bar{b}^2}\right) - 0{,}25\ arctan\frac{1{,}22 \cdot \bar{b} \cdot \sqrt{\sigma}\left(\sqrt{1+1{,}48 \cdot \bar{b}^2 \cdot \sigma} - 0{,}24\right)}{\sqrt{1+1{,}48 \cdot \bar{b}^2 \cdot \sigma} + 0{,}31 \cdot \bar{b}^2 \cdot \sigma}\Big], \quad (32)$$

where $\sigma = \frac{\rho_h}{\rho_s}$ is the ratio of air to water density; $\bar{x} = \frac{x}{b_o}$ is the dimensionless distance located at X from the axis; $\bar{b} = \frac{b}{b_o}$, where bb is the half-width of the water flow at distance X from the axis; b_0 is the initial half-width of the flow.

Since this equation can only be solved approximately, the authors also proposed a simplified relation valid for the interval $0 < \bar{x} < 2500$:

$$\bar{b} = 0{,}16\ \bar{x} \text{ or } b = 0{,}16\ x \quad (33)$$

noting that the error does not exceed 10%.

If we substitute equation (33) into equation (5), which describes the movement of the water flow along the X-axis, we obtain the spreading of the flow at the point X_i in the coordinate system:

$$b = 0{,}16(R \cdot sin\varphi + l_1\ sin(\varphi - \psi)cos\alpha - \vartheta_m\, t + x\,(t_i) + \vartheta_x\,(t_i)\Delta t\ sin\varphi). \quad (34)$$

The spreading of the water flow under different operating conditions is shown as a function of time. The varying spread of the flow over the same time interval is related to the different distances traveled by water droplets. For example, when a droplet is ejected with an initial velocity of 3 m/s, it travels 2.5 m in 0.4 seconds, and its spreading is 0.51 m. At an initial velocity of 5 m/s, the traveled distance is 8.41 m, and the spreading equals 1.35 m.

When distributed over the field surface, the water flow falls onto a plane inclined at an angle αα to the flight direction (Fig.3).

During its motion, the water flow spreads, with its spread points denoted by A, B, C, and D. The point A, which has the smallest value along the Y-axis, contacts the soil surface first. The water flow, with the direction OO_1, intersects the field surface at an angle α.

The value of angle α is determined from the velocities $v_x(t)$ and $V_y(t)$ of the droplet in the XY plane of the coordinate system. The angle αα is expressed as:

$$\text{tg}\,\alpha = \frac{V_y(t)}{V_x(t)} \quad \text{or} \quad \alpha = arctg\ \frac{V_y(t)}{V_x(t)}. \quad (35)$$

In the coordinate system, the spreading of the water flow as a function b=f(x) occurs symmetrically in all directions. The coordinates of the spreading of the water flow relative to point O1 in the XZ plane are determined using the scheme in Fig. 5.

The obtained diagram represents an ellipse. The major and minor axes of the ellipse are determined by the following formulas [8]:

$$2A = \big(0{,}16\ (R \cdot sin\varphi + l_1\ sin(\varphi - \psi)cos\alpha - \ \vartheta_m\, t + x\,(t_i) + \vartheta_x(t_i)\Delta t\ sin\varphi)\big)(tg\alpha + 1), \quad (36)$$

$$2B = \big(0{,}16\ (R \cdot sin\varphi + l_1\ sin(\varphi - \psi)cos\alpha - \ \vartheta_m\, t + x\,(t_i) + \ \vartheta_x(t_i)\Delta t\ sin\varphi)\big). \quad (37)$$

The canonical equation of the ellipse takes the following form:

$$\frac{X^2}{A^2} + \frac{Y^2}{B^2} = 1\,. \tag{38}$$

Where

A=0,08$(R \cdot sin\varphi + l_1\, sin(\varphi - \psi)cos\alpha - \ \vartheta_m\, t + x\,(t_i) + \ \vartheta_x(t_i)\Delta t\ sin\varphi) \cdot (tg\alpha + 1)$;

$B = 0{,}08\ (R \cdot sin\varphi + l_1\, sin(\varphi - \psi)cos\alpha - \ \vartheta_m\, t + x\,(t_i) + \ \vartheta_x(t_i)\Delta t\ sin\varphi) \cdot (ctg\alpha + 1)$.

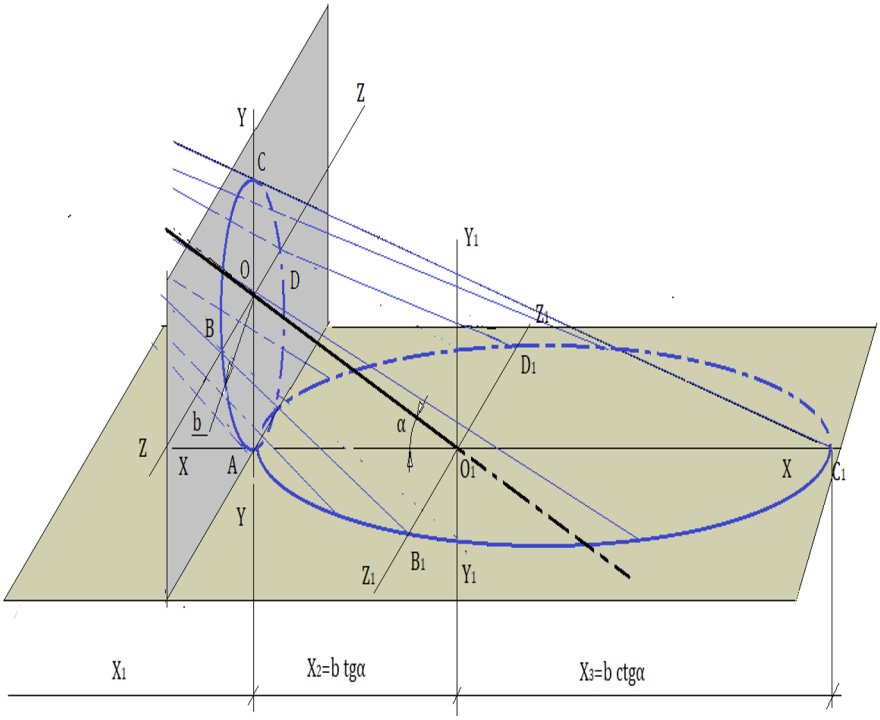

Fig. 4. Scheme of water flow distribution on the field surface during direct-flow sprinkling

The surface of the irrigated field S=π·a·b,

Or, equivalently, it can be expressed by the following formula:

$S = 0{,}0064\ \pi(R \cdot sin\varphi + l_1\, sin(\varphi - \psi)cos\alpha - \ \vartheta_m\, t + \ x\,(t_i) + \vartheta_x(t_i)\Delta t\ \cdot sin\varphi)^2 \cdot (tg\alpha + 1)\ \ (ctg\alpha + 1)$. (39)

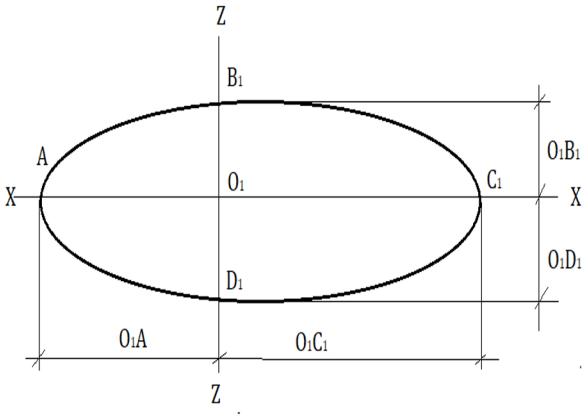

Fig. 5. Epure of water flow distribution on the field surface

The mathematical expressions of the coordinates of water flow distribution on the field surface are defined as follows:

$$X_{\mathrm{A}} = \big(0{,}16\ (R \cdot sin\varphi + l_1\ sin(\varphi - \psi)cos\alpha - \ \vartheta_{\mathrm{m}}\,\mathrm{t} + x\,(t_i) + \vartheta_x(t_i)\Delta t\ sin\varphi)\big)tg\alpha; \quad (40)$$

$$Z_{\mathrm{B1}} = \big(0{,}16\ (R \cdot sin\varphi + l_1\ sin(\varphi - \psi)cos\alpha - \ \vartheta_{\mathrm{m}}\,\mathrm{t} + x\,(t_i) + \vartheta_x(t_i)\Delta t\ sin\varphi)\big)stg\alpha; \quad (41)$$

$$X_{\mathrm{C1}} = 0{,}16\ \ R \cdot sin\varphi + l_1\ sin(\varphi - \psi)cos\alpha - (\ \ \vartheta_m\, t + x\ \ (t_i) + \vartheta_x(t_i)\Delta t\ sin\varphi); \quad (42)$$

$$Z_{\mathrm{D1}} = 0{,}16\ (R \cdot sin\varphi + l_1\ sin(\varphi - \psi)cos\alpha - \ \vartheta_{\mathrm{m}}\,\mathrm{t} + x\,(t_i) + \vartheta_x(t_i)\Delta t\ sin\varphi). \quad (43)$$

Once the water distribution area on the field surface is determined, the irrigation intensity can be calculated using the methods discussed in previous sections.

4 Conclusion

During sprinkler irrigation, the distribution of water droplets over the field surface is one of the decisive factors affecting agricultural crop yield. Uniform and efficient distribution of droplets ensures proper soil moisture levels, delivery of water to the plant root zone, and prevention of water waste. If the water is distributed unevenly, some parts of the field may become over-irrigated while others receive insufficient water. This can negatively affect plant growth and development, increasing the likelihood of reduced yields. When designing and operating sprinkler irrigation systems, it is essential to study the physical and mathematical models of droplet movement, taking into account parameters such as their trajectory, distance, and flight time. This not only contributes to efficient water use but also helps ensure high and stable crop productivity.

Based on the theoretical study of long-distance sprinkler irrigation processes, the following conclusions were made:

- a mathematical model (20) describing the deviation of the water jet from its flow line in direct-flow sprinkling was developed;
- the deviation angle ψ varies within the range ψ=0°÷5.1° depending on the rotation angle φ of the barrel;
- the deviation distance ΔS of the flow line at the point where it meets the field surface ranges between ΔS=0.35–1.6 m.

Mathematical expressions were developed for the coordinates of water droplets falling onto the field surface during direct-flow sprinkling. The obtained results are of scientific and practical importance for designing and improving long-distance sprinkler irrigation systems. Similar analytical and experimental studies on water distribution uniformity are available in the literature [27–31].

Disclosure of Interests. The authors have no competing interests to declare that are relevant to the content of this article.

References

1. Akpasov A.P. Increasing the efficiency of rain formation with substantiation of the design parameters of circular deflector nozzles: Diss. ... Doctor of Technical Sciences. - Saratov, 2018. - P. 141
2. Snipich Yu.F. et al. Theoretical and experimental substantiation of the parameters of the deflector packing. Russian Research Institute of Land Reclamation Problems. https://cyberleninka.ru/article/n/teoreticheskoe-i-yeksperimentalnoe-obosnovanie-parametrov-deflektornoi-nasadki/viewe
3. Isaev A.P. Hydraulics of irrigation machines / A.P. Isaev – M.: Mechanical Engineering, 1973. – 215 p
4. Khudayorov, Z., Mirzakhodjaev, S., Khalilov, R., Nurmikhamedov, B., Mamasov, S. 2023, *E3S Web of Conferences*., 390, 01033 https://doi.org/10.1051/e3sconf/202339001033
5. Khudayorov, Z., Khalilov, R., Mirzakhodjaev, S., Nurmikhamedov, B., Mamasov, S. 2023, *E3S Web of Conferences*, 376, 02013 https://doi.org/10.1051/e3sconf/202337602013
6. Khudayorov, Z., Khalilov, R., Gorlova, I., Mirzakhodjaev, S., Mambetsheripova, A. 2023, *E3S Web of Conferences*, 365, 04011 https://doi.org/10.1051/e3sconf/202336504011
7. Mirzakhodjaev, S., Shodiev, K., Uralov, G., Badalov, S., Choriyeva, D. 2021, *E3S Web of Conferences*, 264, 04047 https://doi.org/10.1051/e3sconf/202126404047
8. Mamatov, F., Mirzaev, B., Mirzahodzhaev, S., Uzakov, Z., Choriyeva, D. 2021, *IOP Conference Series: Materials Science and Engineering*, 1030(1), 012164 DOI: 10.1088/1757-899x/1030/1/012164
9. Mirzaev, B., Mamatov, F., Ergashev, I., ...Kodirov, U., Ergashev, G. 2019, *E3S Web of Conferences*, 135, 01065 https://doi.org/10.1051/e3sconf/201913501065
10. Akhmetov, A.A., Allanazarov, M.A., Rakhimboyeva, D.S., Rajabov, I.R. 2024, *AIP Conference Proceedings*, 3045(1), 040008 https://doi.org/10.1063/5.0198816
11. Akhmetov, A.A., Akhmedov, Sh.A., Allanazarov, M.A., Asamov, R.H. 2023, *IOP Conference Series: Earth and Environmental Science*, 1138(1), 012047 doi:10.1088/1755-1315/1138/1/012047

12. Zhanikulov, S., Khalmuradov, T., Allanazarov, M. 2022, *IOP Conference Series: Earth and Environmental Science*, 1112(1), 012015 DOI 10.1088/1755-1315/1112/1/012015
13. Akhmetov, A.A., Allanazarov, M.A., Muratov, L.B., Kambarova, D.U. 2021, *IOP Conference Series: Earth and Environmental Science*, 868(1), 012075
14. Irgashev, A., Ishmuratov, Kh.K., Allanazarov, M.A., Ishmuratova, K.Kh. 2021, *IOP Conference Series: Earth and Environmental Science*, 868(1), 012068
15. Obidov, A., Nuriev, K., Allanazarov, M., Kurbonov, E., Khudoyberdiev, R. 2021, *E3S Web of Conferences*, 284, 02012 https://doi.org/10.1051/e3sconf/202128402012
16. Eshpulatov, N., Khalmuradov, T., Khalilov, R., Obidov, A., Allanazarov, M. 2021, *E3S Web of Conferences*, 264, 04072 https://doi.org/10.1051/e3sconf/202126404072
17. Eshpulatov, N., Khalmuradov, T., Khalilov, R., ...Nurmanov, S., Omonov, D. 2021, *E3S Web of Conferences*, 264, 04086
18. Ashirov, M., Omonov, D., Khalilov, R., Rakhimov, U. 2021, *E3S Web of Conferences*, 244, 02018 https://doi.org/10.1051/e3sconf/202124402018
19. Farmonov, E., Lakaev, S., Khalilov, R., Gorlova, I. 2020, *IOP Conference Series: Materials Science and Engineering*, 883(1), 012097
20. Djiyanov, M., Xalilov, R., Isakova, F. 2024, *BIO Web of Conferences*, 85, 01034 https://doi.org/10.1051/bioconf/20248501034
21. Djiyanov, M., Tadjibekova, I., Temirkulova, N., Kholmuradov, O. 2024, *Lecture Notes in Networks and Systems*, 733, 565–571
22. Djiyanov, M., Tadjibekova, I., Temirkulova, N. 2022, *IOP Conference Series: Earth and Environmental Science*, 1068(1), 012004 doi:10.1088/1755-1315/1068/1/012004
23. Isakova, F., Tadjibekova, I., Kurbonov, F. 2024, *BIO Web of Conferences*, 85, 01037 https://doi.org/10.1051/bioconf/20248501037
24. Astanakulov, K., Kurbonov, F., Isakova, F. 2023, *E3S Web of Conferences*, 381, 01001 https://doi.org/10.1051/e3sconf/202338101001
25. Irisov, K., Gorlova, I., Khudaev, I. 2024, *BIO Web of Conferences*, 105, 01016 https://doi.org/10.1051/bioconf/202410501016
26. Aslonov, N., Irisov, K. 2023, *E3S Web of Conferences*, 390, 01032 https://doi.org/10.1051/e3sconf/202339001032
27. Irisov, K., Xamidov, G. 2023, *E3S Web of Conferences*, 386, 03003 https://doi.org/10.1051/e3sconf/202338603003
28. Irisov, K.D., Bekmurodov, I.R. 2023, *IOP Conference Series: Earth and Environmental Science*, 1284(1), 012041 DOI 10.1088/1755-1315/1284/1/012041
29. Irisov, K.D., Akhmedov, D.A., Aliboyev, B.A. 2022, *IOP Conference Series: Earth and Environmental Science*, 1076(1), 012011 DOI 10.1088/1755-1315/1076/1/012011
30. Irisov, Kh.D., Botirov, R.M., Khudoykulov, R.F. 2021, *IOP Conference Series: Earth and Environmental Science*, 868(1), 012001 DOI 10.1088/1755-1315/868/1/012001
31. Irisov, Kh.D., Olimjonov, R.Z. 2021, *IOP Conference Series: Earth and Environmental Science*, 868(1), 012034 DOI 10.1088/1755-1315/868/1/012034

Open Access This chapter is licensed under the terms of the Creative Commons Attribution-NonCommercial 4.0 International License (http://creativecommons.org/licenses/by-nc/4.0/), which permits any noncommercial use, sharing, adaptation, distribution and reproduction in any medium or format, as long as you give appropriate credit to the original author(s) and the source, provide a link to the Creative Commons license and indicate if changes were made.

The images or other third party material in this chapter are included in the chapter's Creative Commons license, unless indicated otherwise in a credit line to the material. If material is not included in the chapter's Creative Commons license and your intended use is not permitted by statutory regulation or exceeds the permitted use, you will need to obtain permission directly from the copyright holder.